Available online at www.sciencedirect.com
ScienceDirect
Trans. Nonferrous Met. Soc. China 28(2018) 1166−1175
Transactions of Nonferrous Metals Society of China
www.tnmsc.cn

Property alterations of Sn−0.6Cu−0.05Ni−Ge lead-free solder by Ag, Bi, In and Sb addition

Kannachai KANLAYASIRI, Rachata KONGCHAYASUKAWAT

Department of Industrial Engineering, Faculty of Engineering,
King Mongkut's Institute of Technology Ladkrabang, Bangkok 10520, Thailand

Received 5 May 2017; accepted 26 August 2017

Abstract: The Sn−Cu−Ni−Ge solder is a strong challenger to the Sn−Ag−Cu (SAC) solders as a replacement for the Sn−Pb eutectic solder. This research investigated the effects of addition of Ag, Bi, In, and Sb on the physical properties of the Sn−0.6Cu−0.05Ni−Ge (SCNG) lead-free solder and the interfacial reaction with the Cu substrate. The melting behavior, microstructure, tensile strength, and wettability of the SCNG−x (x=Ag, Bi, In, Sb) solders were examined. The findings revealed that the introduction of Ag, Bi, In, and Sb minimally altered the solidus temperature, liquidus temperature, and tensile strength of the solder. However, the cooling behavior and solidified microstructure of the solder were affected by the concentration of the alloying elements. The wettability of the SCNG solder was improved with the doping of the alloying elements except Sb. The thickness of intermetallic layer was increased by the addition of the alloying elements and was related to the cooling behavior of the solder. The morphology of intermetallic layer between the SCNG−x solders and the Cu substrate was different from that of the typical SAC solders. In conclusion, alloying the SCNG solder with Ag, Bi, In or Sb is able to improve particular properties of the solder.
Key words: Sn−Cu−Ni−Ge solder; lead-free solder; alloying effect; physical properties

1 Introduction

The growing environmental concerns and related laws and regulations, e.g., the Restriction of Hazardous Substances (RoHS) Directive, have contributed to the development of many lead-free solders to replace the lead-containing solders, particularly the Sn−Pb solders. The most widely used lead-free solders in the industry are the Sn−Ag−Cu (SAC) solders group because of their good solderability, high electrical conductivity, and high joint strength [1,2]. However, the SAC solders possess a higher melting temperature vis-à-vis the Sn−Pb eutectic solder (183 ^{o}C) and their soldered joints are prone to crack due to the presence of the brittle Ag_3Sn intermetallic phase [3,4]. Moreover, the SAC solders are costlier due to the high Ag content and the surface of the soldered joints is dull [1,5,6].

The Sn−Cu−Ni−Ge lead-free solder (or SN100C) is a strong challenger for market share of the SAC solders as a replacement for the Sn−Pb eutectic solder. The Sn−Cu−Ni−Ge solder is an improved version of the low-cost Sn−Cu (SC) eutectic solder by doping only a small amount of Ni and Ge. Specifically, the introduction of Ni contributes to the more refined microstructure of the solder and the more stable Cu_6Sn_5 intermetallic phase of the soldered joint [7−9]. Ni also reduces the corrosion of Cu on the print circuit board [10]. Meanwhile, a very small addition of Ge lowers the oxidation and prevents bridging during soldering while improving the wettability of the solder [11,12]. However, the Sn−Cu−Ni−Ge solder exhibits a relatively high melting temperature.

The physical properties of a solder can be enhanced by alloying with certain elements, such as Ag, Al, Bi, Co, Ga, In, La, and Sb. These alloying elements nevertheless improve some physical properties of the solder at the expense of other properties, and the effects of different alloying elements on the solder alloy vary greatly [13−26]. Meanwhile, existing research studies on the effects of variable alloying elements have focused mostly on the generic lead-free solders, such as the SC and SAC, while those involving the Sn−Cu−Ni−Ge solders are very limited [13−28].

This research thus investigated the effects of low-concentration Ag, Bi, In, and Sb on the physical

Corresponding author: Kannachai KANLAYASIRI; Tel: +66-2-3298339; Fax: +66-2-3298340; E-mail: kkkannac@kmitl.ac.th
DOI: 10.1016/S1003-6326(18)64754-5

properties of the Sn−0.6Cu−0.05Ni−Ge (SCNG) lead-free solder, including the melting behavior, microstructure, tensile strength, and wettability. The formation of the interfacial layer between the SCNG−x (x=Ag, Bi, In, Sb) solders and the Cu substrate was also investigated.

2 Experimental

In this research, the SCNG base solder was fabricated from four basic elements: Sn, Cu, Ni, and Ge. The alloying elements (i.e., Ag, Bi, In, and Sb) of 0.05% or 0.10% (mass fraction) were then individually introduced into the base solder. The alloying elements were intended to introduce at low concentrations to avoid the domination of the effects of these elements over those of Ni and Ge. Table 1 lists the nominal compositions of the experimental SCNG−x solders.

Table 1 Nominal compositions of experimental SCNG−x solders

Solder	Mass fraction/%							
	Cu	Ni	Ge	Ag	Bi	In	Sb	Sn
SCNG	0.60	0.05	0.005	−	−	−	−	Bal.
SCNG+0.05Ag	0.60	0.05	0.005	0.05	−	−	−	Bal.
SCNG+0.10Ag	0.60	0.05	0.005	0.10	−	−	−	Bal.
SCNG+0.05Bi	0.60	0.05	0.005	−	0.05	−	−	Bal.
SCNG+0.10Bi	0.60	0.05	0.005	−	0.10	−	−	Bal.
SCNG+0.05In	0.60	0.05	0.005	−	−	0.05	−	Bal.
SCNG+0.10In	0.60	0.05	0.005	−	−	0.10	−	Bal.
SCNG+0.05Sb	0.60	0.05	0.005	−	−	−	0.05	Bal.
SCNG+0.10Sb	0.60	0.05	0.005	−	−	−	0.10	Bal.

An optical emission spectrometer (Thermo, ARL 3460) was used to examine the composition of the specimens, and the effects of Ag, Bi, In, and Sb on the microstructure, tensile strength, melting temperature, wettability, and oxidation resistance were then determined. In addition, a differential scanning calorimeter (Netzsch DSC 204 F1 Phoenix), operated at a heating rate of 10 °C/s under the N_2 atmosphere, was used to measure the melting temperature of the SCNG−x alloys. The wettability of the SCNG−x solders on the Cu substrate was measured in terms of the spread factor according to the JIS Z3198−3 standard. The wettability test using RMA flux was performed at 260 °C for 30 s. The specimens were then left in ambient temperature to cool down. The Cu substrate for the wettability test was the oxygen-free high conductivity copper plate with dimensions of 30 mm × 30 mm × 0.35 mm and the arithmetic surface roughness R_a of 0.06 μm. Figure 1 illustrates the schematic shape of a soldered joint, and the spread factor (S_f) was calculated using Eq. (1), where D is the joint diameter and H is the joint height.

$$S_f = \frac{D-H}{H}\times 100\% \quad (1)$$

The tensile strength of the SCNG−x solders was determined according to the ASTM E8M standard, using Shimadzu's Autograph AG-X with a capacity of 100 kN. The microstructure of the SCNG−x solders was examined using a scanning electron microscope (SEM, JEOL JSM−6610LV) coupled with the Oxford link ISIS series 300 energy dispersive X-ray spectroscopy (EDX) to determine the chemical contents of phases. An X-ray diffractometer (Bruker D8 Discover) was used to identify the crystalline structure of phases. The thickness of the intermetallic layer at the interface between the solder and the Cu substrate was determined by dividing the area of the intermetallic phase by its measured length. The Image Pro® Express software was used to determine the area and the measured length of the intermetallic phase.

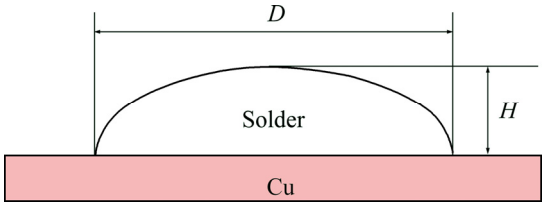

Fig. 1 Schematic of soldered joint for wettability test

3 Results and discussion

3.1 Melting behavior

The melting behavior of the SCNG−x solders was determined in terms of the solidus temperature and liquidus temperature. Figure 2 shows DSC thermograms of the SCNG−x specimens during heating (H) and cooling (C). The solidus and liquidus temperatures of the SCNG base solder were about 230 and 233 °C, respectively. The introduction of an alloying element slightly altered the solidus temperature and the liquidus temperature of the SCNG solder as illustrated in Fig. 3. In general, the changes in the solidus and liquidus temperatures could be attributed to the ability of the alloying elements to shift the alloy composition closer or further away from the eutectic composition [29]. In this experiment, although the introduction of an alloying

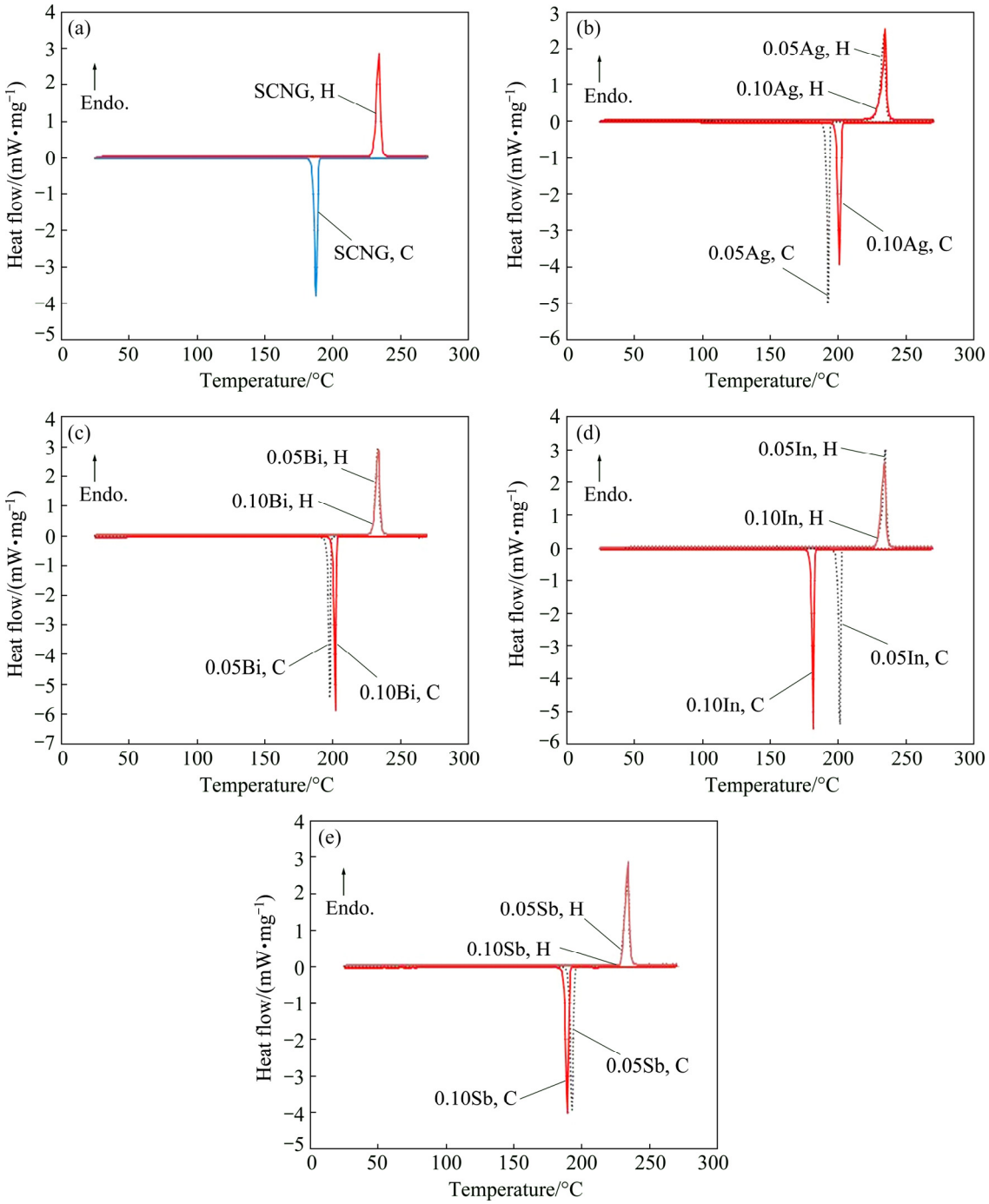

Fig. 2 DSC thermograms of SCNG−x specimens (H: Heating; C: Cooling): (a) SCNG; (b) SCNG−Ag; (c) SCNG−Bi; (d) SCNG−In; (e) SCNG−Sb

element did not significantly change the solidus and liquidus temperatures of the SCNG solder, the addition of an alloying element clearly affected the cooling behavior of the solder as displayed in Fig. 2. For example, in Fig. 2(d), the peak of the cooling thermogram was shifted by about 15 °C when 0.05% In was introduced. In addition, the alteration of cooling behavior led to microstructural changes of the solder as discussed in the next section.

3.2 Microstructure

The microstructure of the SCNG solder comprised the β-Sn phase and the eutectic structure as illustrated in Fig. 4. In Fig. 4(a), the β-Sn phase, as represented by the light area, is of dendritic shape, while the dark area represents the eutectic structure of the β-Sn and intermetallic phases. The average cross sectional area of dentritic arms of the β-Sn phase was 78.9 μm^2. The EDS and XRD analyses indicated Cu_6Sn_5 intermetallic phase

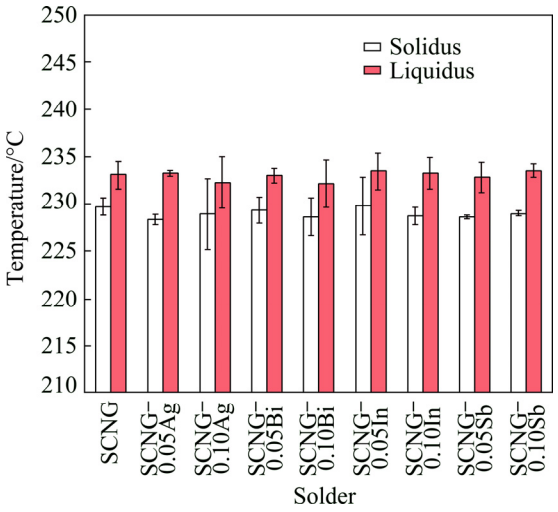

Fig. 3 Solidus and liquidus temperatures of SCNG−x solders

in the eutectic area as shown in Figs. 4(c), (d) and (e). The crystal structure of Cu_6Sn_5 found in this study was base-centered monoclinic (η'-Cu_6Sn_5). The lattice parameters of the intermetallic phase were a=1.1022 nm, b=0.7282 nm, c=0.9827 nm, α=90.00°, β=98.84°, and γ=90.00°, corresponding to $C2/c$ space group. However, with the presence of small amount of Ni as shown in Fig. 4(d), the $(Cu, Ni)_6Sn_5$ intermetallic phase might exist in the eutectic area due to the complete solubility of Ni in Cu and both intermetallic phases have the same crystal structure [30]. The information on the transformation of these intermetallic phases is limited and thereby warrants further investigation.

Figure 5 illustrates the microstructures of the SCNG solder doped with 0.05% Ag and 0.10% Ag. The β-Sn phase became larger and more dendritic, in comparison

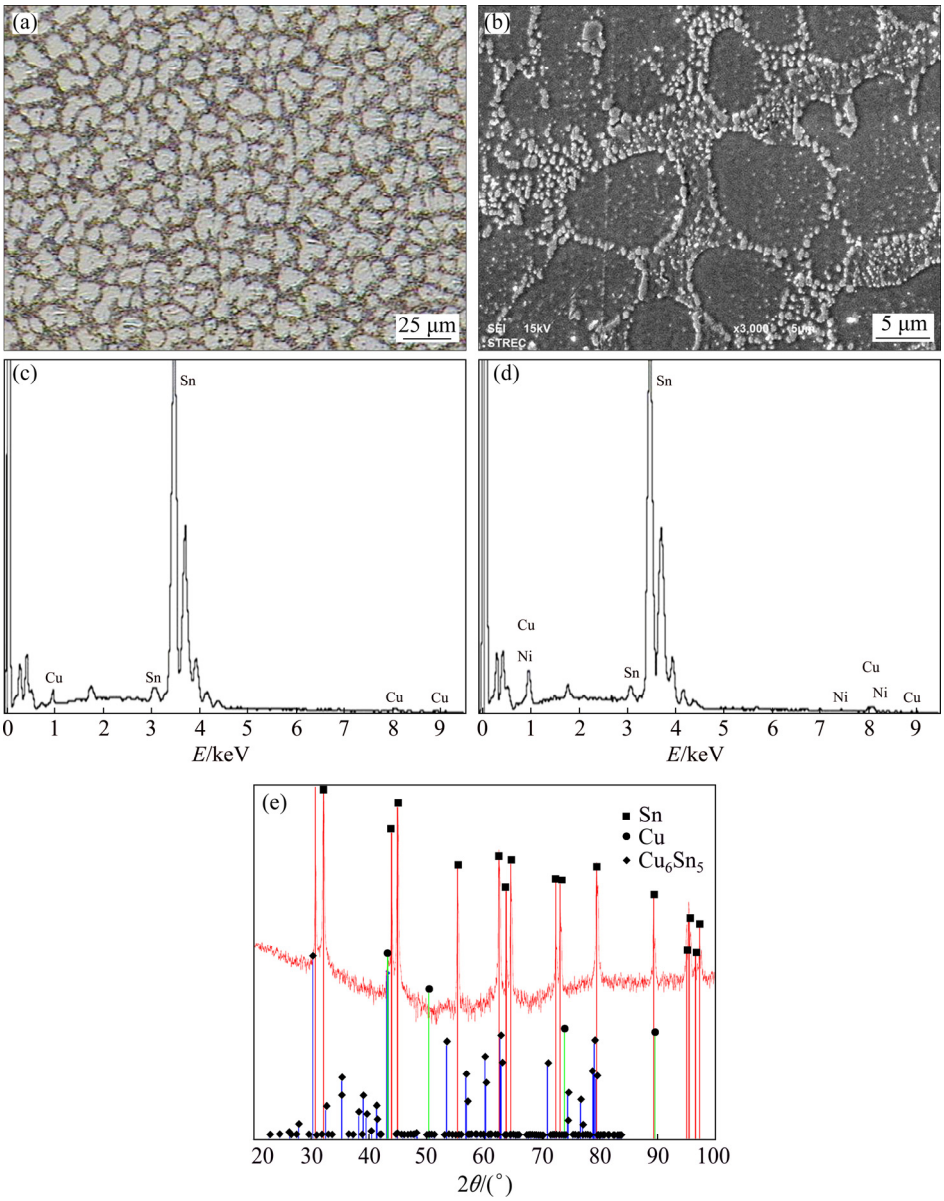

Fig. 4 Microstructures and corresponding EDS and XRD analyses of SCNG solder: (a) Optical micrograph; (b) SEM micrograph; (c, d) EDS spectra of eutectic area; (e) XRD pattern

with Fig. 4, and the intermetallic phase in the eutectic area was Cu_6Sn_5. The average cross sectional areas of dentritic arms of β-Sn of the SCNG−0.05Ag and SCNG−0.10Ag were 118.4 and 124.2 μm^2, respectively. The size of the β-Sn phases was related to the cooling behavior of the solders. As illustrated in Fig. 2(b), during cooling of each alloy, the SCNG−0.10Ag was completely solidified about 9 °C higher than that of the SCNG−0.05Ag. Thus, with the earlier solidification, the size of the β-Sn phase of the SCNG−0.10Ag was larger than that of the SCNG−0.05Ag. The findings are consistent with HUH et al [31], who documented that the introduction of Ag into the Sn−Cu eutectic solder, given the concentration below 0.10%, contributed to the enlargement of the β-Sn phase. In this research, despite the presence of Ag in the solders, no Ag_3Sn intermetallic phase was detected, probably due to the low concentrations of Ag in the solders. The absence of Ag_3Sn will provide a more reliable solder joint when the solder is used with electronics components.

The introduction of Bi reduced the size of β-Sn phase of the SCNG, as shown in Fig. 6. The shape of β-Sn was nevertheless still dendritic. In fact, the average sizes of β-Sn phase of the Bi-doped SCNG solders were the smallest among the experimental SCNG−x solders. The average cross sectional areas of dentritic arms of β-Sn in the SCNG−0.05Bi and SCNG−0.10Bi were 44.9 and 59.0 μm^2, respectively. Similar to the SCNG−Ag solders, the size of β-Sn phases was correlated to the cooling behavior of SCNG−Bi alloys as shown in Fig. 2(c). The SCNG−0.05Bi solidified later than the SCNG−0.10Bi, resulting in a smaller β-Sn phase. The reduced β-Sn size due to the addition of Bi is consistent with the results obtained by KARIYA and OTSUKA [32], who introduced Bi into the SnAg solder. The intermetallic phase in the eutectic area was Cu_6Sn_5. No precipitate of Bi particles was detected because the Bi concentrations were far lower than the solubility limit of Bi at room temperature in the Sn matrix [33].

Figure 7 depicts the microstructures of the SCNG−0.05In and SCNG−0.10In. The shape of β-Sn was noticeably dendritic. However, no intermetallic phase of In was detected, but only Cu_6Sn_5 was present. The average cross sectional areas of dentritic arms of β-Sn were 77.7 and 56.1 μm^2 for the SCNG−0.05In and SCNG−0.10In, respectively. Likewise, the size of β-Sn phases of SCNG−In alloys was associated to the cooling behavior of the alloys as displayed in Fig. 2(d). The solidification of SCNG−0.05In was completed about 20 °C higher than that of SCNG−0.10In, resulting in a larger size of β-Sn phase. In this research, the decrease in the β-Sn grain size subsequent to the introduction of In is consistent with our previous study [18].

Figure 8 illustrates the microstructures of the SCNG−0.05Sb and SCNG−0.10Sb. The intermetallic phase in the eutectic area was Cu_6Sn_5. The average cross

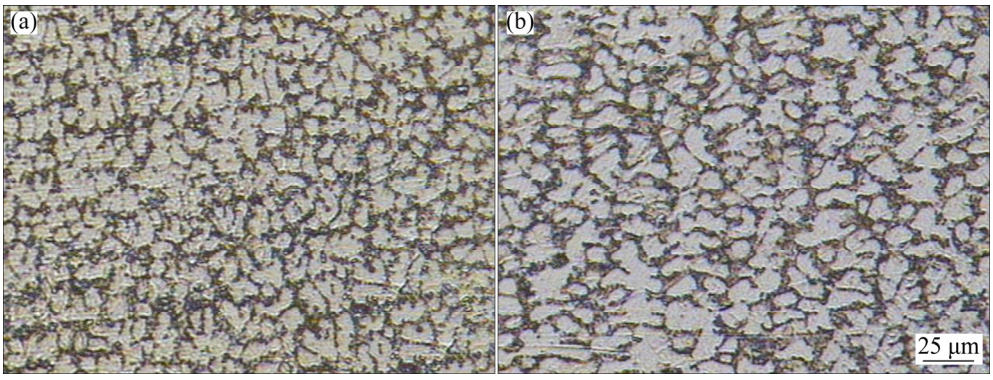

Fig. 5 Microstructures of SCNG−0.05Ag (a) and SCNG−0.10Ag (b)

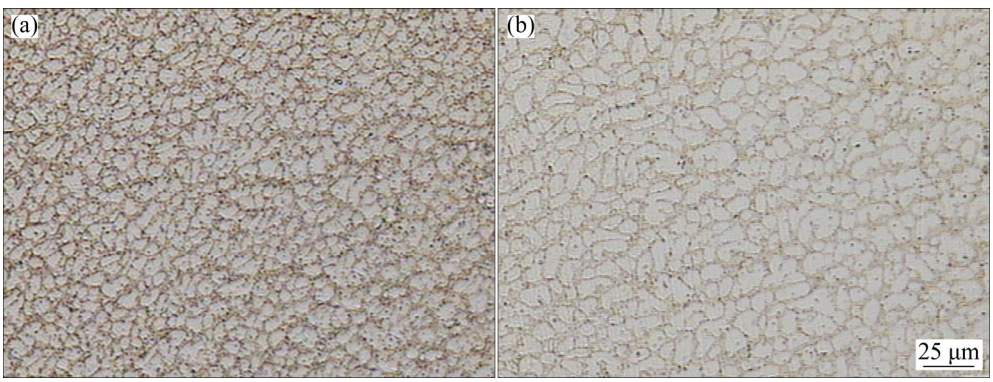

Fig. 6 Microstructures of SCNG−0.05Bi (a) and SCNG−0.10Bi (b)

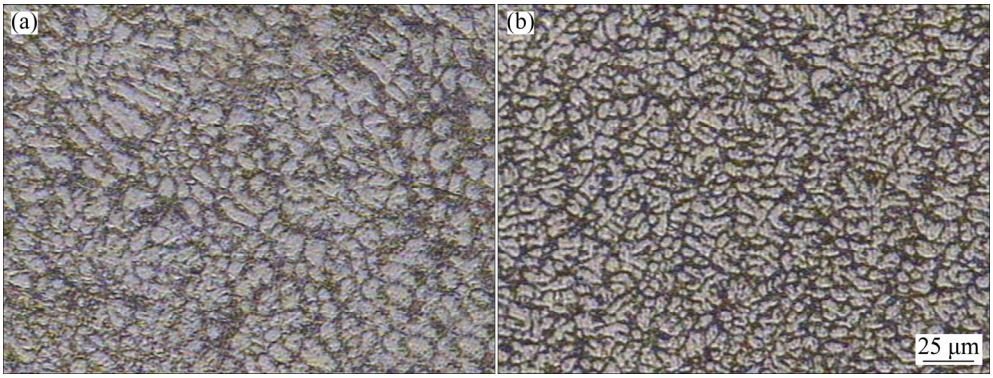

Fig. 7 Microstructures of SCNG−0.05In (a) and SCNG−0.10In (b)

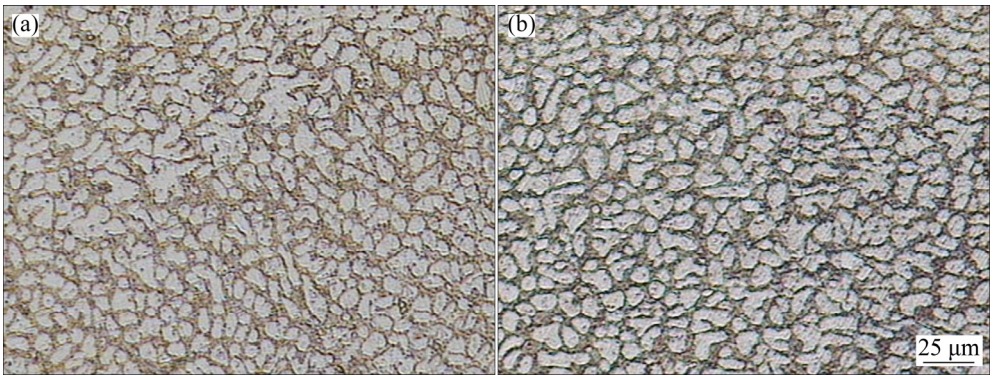

Fig. 8 Microstructures of SCNG−0.05Sb (a) and SCNG−0.10Sb (b)

sectional area of dentritic arms of β-Sn decreased as Sb content increased, with the average cross sectional areas of dentritic arms of β-Sn for the SCNG−0.05Sb and SCNG−0.10Sb of 67.1 and 62.3 μm^2, respectively. The size of β-Sn phases of SCNG−Sb also corresponded to the cooling thermograms as displayed in Fig. 2(e). The solidification temperature of SCNG−0.10Sb was lower than that of SCNG−0.05Sb, leading to a smaller β-Sn phase. The refinement effect of Sb on the β-Sn phase was consistent with the results obtained by EL-DALY et al [23,34], who applied Sb to refine the microstructure of the Sn−Ag−Cu and Sn−Zn solder alloys.

3.3 Tensile strength and fracture behaviors

The tensile strength of the SCNG−x solders was determined in accordance with the ASTM E8M standard, and the results are shown in Fig. 9. The tensile strength of the solders was not clearly different under the selected concentrations of the alloying elements. Based on the analysis of variance with the 95% confidence level, the tensile strengths of the variable SCNG−x solders were not significantly different. In the tensile test, all of the SCNG−x specimens exhibited the necking phenomenon, indicating the development of a ductile fracture. Figure 10 depicts the fractographs of the fractured surfaces, with the dimples on the fractured surfaces confirming the ductile fracture of the SCNG−x specimens. The findings showed that the alloying elements minimally altered the fracture behaviors of the SCNG solder.

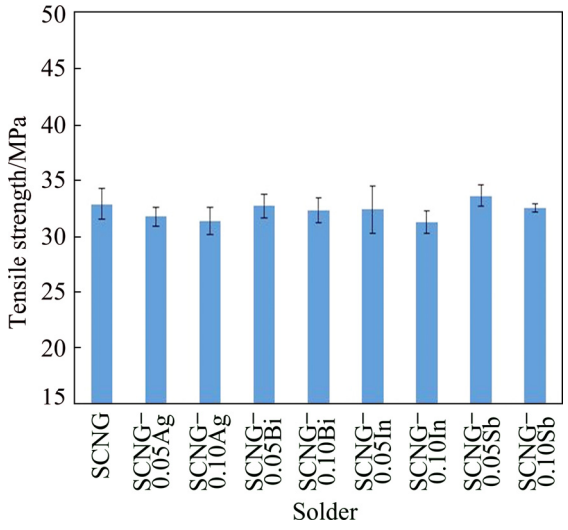

Fig. 9 Tensile strength of SCNG−x solders

3.4 Wettability

As illustrated in Fig. 11, all of the alloying elements except Sb improved the wettability of the SCNG solders on the Cu substrate. The spread factor (S_f) of the solder increased in response to the introduction of Ag, Bi or In. Specifically, the higher content of the alloying element contributed to the greater spread factor. Since in this

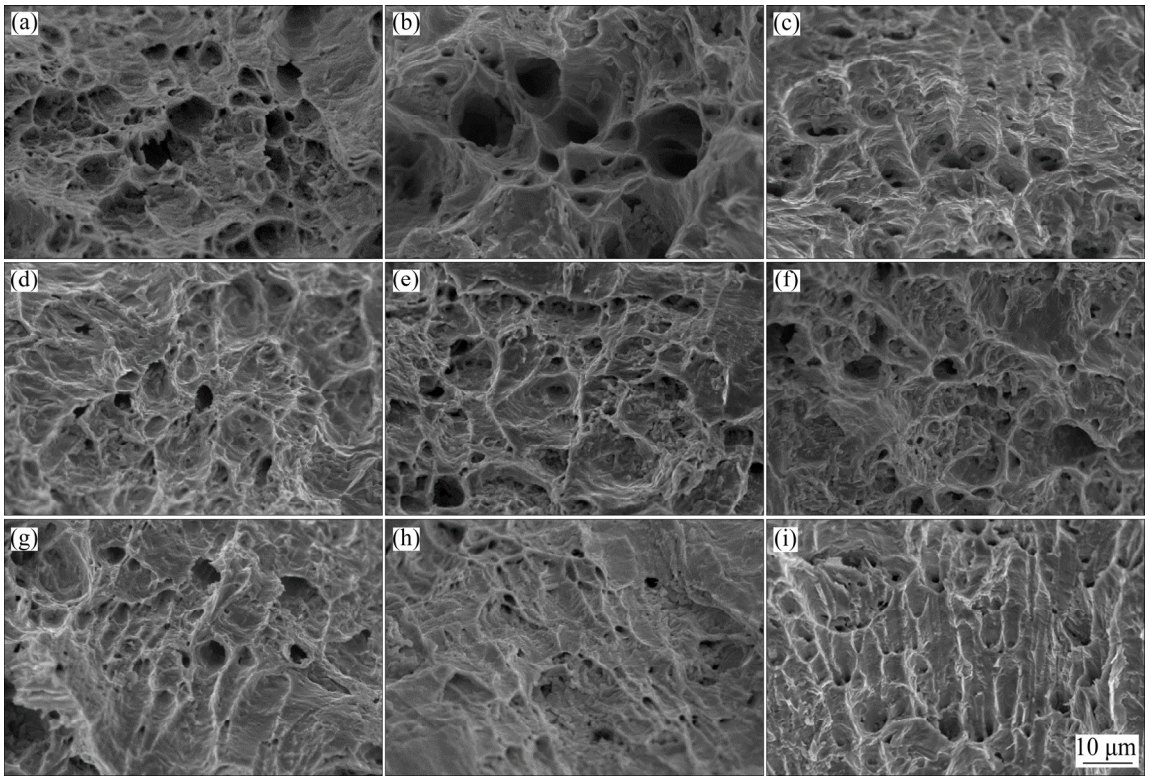

Fig. 10 Fractographs of SCNG−x specimens: (a) SCNG; (b) SCNG−0.05Ag; (c) SCNG−0.10Ag; (d) SCNG−0.05Bi; (e) SCNG−0.10Bi; (f) SCNG−0.05In; (g) SCNG−0.10In; (h) SCNG−0.05Sb; (i) SCNG−0.10Sb

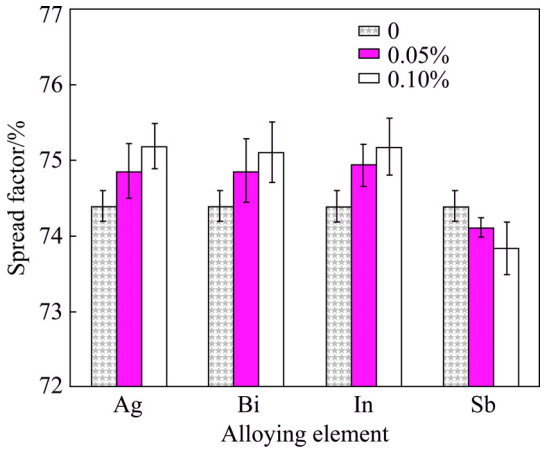

Fig. 11 Effects of alloying elements on spread factor of SCNG solder

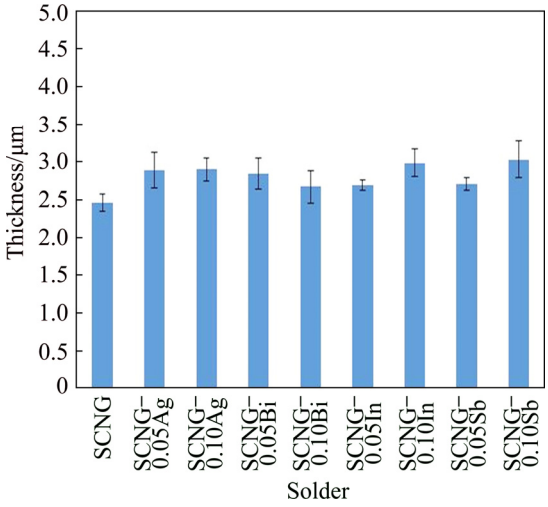

Fig. 12 Thicknesses of intermetallic layer between SCNG−x and Cu substrate

study the alloying elements did not lower the liquidus temperature of the SCNG solder, it indicated that the alloying elements reduced the surface tension of the molten solder or enhanced its fluidity, resulting in the improvement of the wettability. In contrast, Sb deteriorated the wettability of the SCNG solder, and the higher Sb content resulted in the lower wettability.

3.5 Interfacial layer

In Fig. 12, all the alloying elements slightly increased the thickness of the interfacial layer between the solder and the Cu substrate. The intermetallic phase at the interface was Cu_6Sn_5 in all specimens. The crystal structure of Cu_6Sn_5 found was base-centered monoclinic (η'-Cu_6Sn_5). As mentioned earlier, with the presence of Ni as shown in Fig. 13(b), $(Cu, Ni)_6Sn_5$ could be present at the interface as well. This is attributable to the higher thermodynamics affinity of Ni and Sn than that of Cu and Sn and the complete solubility of Ni in Cu [35]. Thus, $(Cu,Ni)_6Sn_5$ with higher phase stability was formed at the interface rather than the lower stability

Cu_6Sn_5. Figures 13(a) and (b) respectively illustrate the intermetallic layer of the SCNG and the Cu substrate and its EDS spectrum. The thickness of the intermetallic layer was 2.46 μm and slightly increased with the introduction of the alloying element. The thickness increase of intermetallic layers was in the range of 0.21−0.57 μm, depending on the alloying element added.

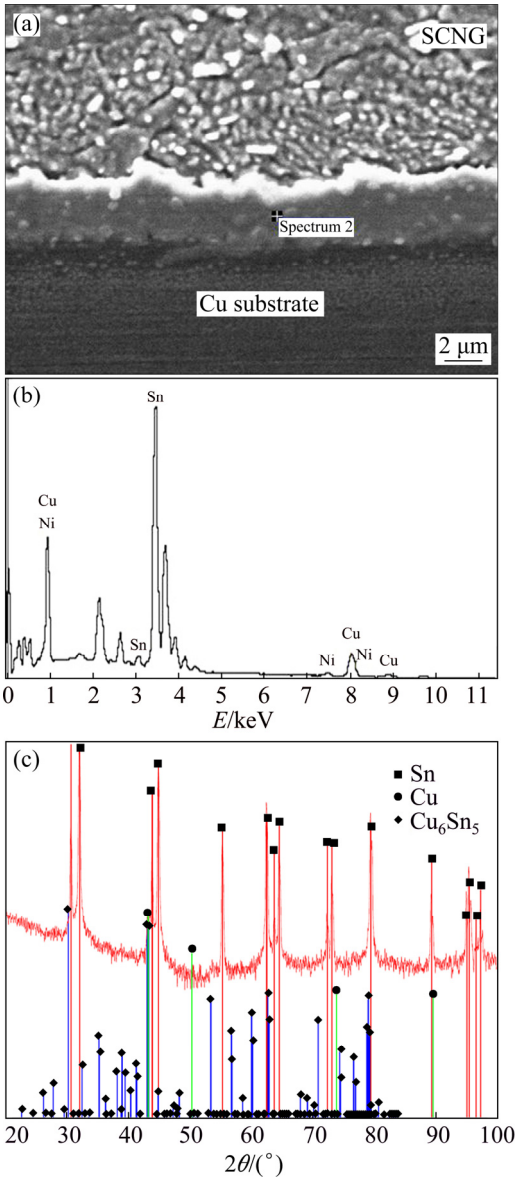

Fig. 13 Interfacial layer of SCNG and Cu substrate (a), EDS spectrum (b) and XRD pattern (c)

The thickness of intermetallic layers of alloyed solders was related to the cooling behavior of the solder as previously shown in Fig. 2. With the same alloying element, the solder that completely solidified at a higher temperature provided a thinner intermetallic layer at the interface because of shorter reaction time between the molten solder and Cu substrate. After the solidification, the interfacial reaction in solid state occurred at a much lower rate than that in liquid state of the solder, resulting in a thinner intermetallic layer.

In light of the fact that the morphology of the intermetallic layer is critical to the joint strength [36−39], it should be mentioned that in this research, the morphology of the intermetallic layer was relatively uniform (Fig. 13(a)) while the morphologies of intermetallic layers of the typical SC and SAC solders were of finger-like or scallop shape [40−43]. The uniform intermetallic layer in this research is consistent with the SC−Ni solder in Refs. [44,45] and the SAC−Ni−Ge solder in Refs. [46,47]. However, no discussion about the formation of the uniform intermetallic layer was provided in both studies.

The formation of the uniform intermetallic layer could be attributed to Ni as the vital element promoting the uniformity of the intermetallic layer. Specifically, Ni atoms distributed in $(Cu,Ni)_6Sn_5$ might act as a nucleation catalyst for the intermetallic phase during the solidification producing the finer intermetallic grains, and thus resulting in a more uniform intermetallic layer [43,48]. This explanation is verified by the experimental results on the Sn−Cu−Co solder of PIYAVATIN et al [26], the Sn−Ag−Co solder of GAO et al [35], and the SAC−Fe, SAC−Co, SAC−Ni solders of WANG et al [49]. It is evident that when an alloying element, e.g., Co, Fe, and Ni, is introduced into a solder, such an alloying element would act as the nucleation catalyst for the formation of the intermetallic grains, resulting in a more uniform intermetallic layer. The intermetallic layers in Refs. [26,35,49] are also uniform.

Finally, the experimental results from this research were compared to the original properties of the SCNG in terms of general requirements for the lead-free solders as presented in Table 2. It is clear that alloying the SCNG solder with Ag, Bi, In or Sb is able to improve particular properties of the solder.

Table 2 Comparison of properties of SCNG−x solders with original SCNG solder

Property	Requirement	Results from this research compared to original SCNG
Thermal behavior	Low solidus and liquidus temperatures; short solidification time	Similar solidus and liquidus temperatures; shorter solidification time (except In)
Mechanical behavior	High tensile strength; ductile fracture	Similar tensile strength and fracture mode (ductile fracture)
Wettability	Low contact angle	Lower contact angle (except Sb)
Intermetallic layer	Thin IMC layer	Similar IMC thickness

4 Conclusions

This research investigated the effects of Ag, Bi, In, and Sb on the melting behavior, microstructure, tensile strength, and wettability of the SCNG solder. In addition, the intermetallic layer between the SCNG−x solders and the Cu substrate was studied. The findings revealed that the introduction of the alloying elements into the SCNG base solder had an effect on the average size of β-Sn but minimal impact on the tensile strength of the alloys. Furthermore, the alloying elements had a minimal effect on the solidus temperature and the liquidus temperature of the SCNG solder. Except for Sb, the wettability of the SCNG solder was improved with the addition of Ag, Bi, and In. Meanwhile, the intermetallic layer formed between the SCNG−x solders and the Cu substrate was of uniform morphology, unlike that of the typical SAC solders. In addition, the thickness values of the intermetallic layer were closely related to the cooling behavior of molten SCNG−x solders.

Acknowledgments

The authors would like to thank King Mongkut's Institute of Technology Ladkrabang and the National Research Council of Thailand for the financial sponsorship of this project.

References

[1] ABTEW M, SELVADURAY G. Lead-free solders in microelectronics [J]. Materials Science and Engineering R, 2000, 27: 95−106.

[2] SHANGGUAN D. Lead-free solder interconnect reliability [M]. Ohio: ASM International, 2005.

[3] CHEW K H, PANG J H L. Impact of drop-in lead free solders on microelectronics packaging [C]//Proceedings of Electronics Packaging Technology Conference. Singapore: IEEE, 2005: 451−454.

[4] AMAGAI M, TOYODA Y, OHNISHI T, AKITA S. High drop test reliability: lead-free solders [C]//Proceedings of Electronic Components and Technology Conference. Las Vegas, Nevada: IEEE, 2004: 1304−1309.

[5] ZENG G, XUE S, ZHANG L, GAO L. Recent advances on Sn−Cu solders with alloying elements: Review [J]. Journal of Materials Science: Materials in Electronics, 2011, 22: 565–578.

[6] KIM K S, SUGANUMA K. Development of new Sn−Ag−Cu lead-free solders containing fourth elements [C]//Proceedings of the 3rd International Symposium on Environmentally Conscious Design and Inverse Manufacturing. Tokyo: IEEE, 2003: 414−415.

[7] DONG W, SHI Y, LEI Y, XIA Z, GUO F. Effects of small amounts of Ni/P/Ce element additions on the microstructure and properties of Sn3.0Ag0.5Cu solder alloy [J]. Journal of Materials Science: Materials in Electronics, 2009, 20: 1008−1017.

[8] NOGITA K, NISHIMURA T. Nickel-stabilized hexagonal $(Cu, Ni)_6Sn_5$ in Sn−Cu−Ni lead-free solder alloys [J]. Scripta Materialia, 2008, 59: 191−194.

[9] NOGITA K, McDONALD S D, TSUKAMOTO H, READ J, SUENAGA S, NISHIMURA T. Inhibiting cracking of interfacial Cu_6Sn_5 by Ni additions to Sn-based lead-free solders [J]. Transactions of the Japan Institute of Electronics Packaging, 2009, 2: 46−54.

[10] HANDWERKER C, KATTNER U, MOON K W. Lead-free soldering [M]. New York: Springer, 2007: 21−74.

[11] HABU K, TAKEDA N, WATANABE H, OOKI H, ABE J, SAITO T, TANIGUCHI Y, TAKAYAMA K. Development of lead-free solder alloys of the Ge doped Sn−Ag−Bi system [C]//Proceedings of the 1st International Symposium on Environmentally Conscious Design and Inverse Manufacturing. Tokyo: IEEE, 1999: 606−609.

[12] YEN Y W, CHIANG Y C, JAO C C, LIAW D W, LO S C, LEE C. Interfacial reactions and mechanical properties between Sn−4.0Ag−0.5Cu and Sn−4.0Ag−0.5Cu−0.05Ni−0.01Ge lead-free solders with the Au/Ni/Cu substrate [J]. Journal of Alloys and Compounds, 2011, 509: 4595−4602.

[13] ZHOU Y, PAN Q, HE Y, LIANG W, LI W, LI Y, LU C. Microstructures and properties of Sn−Ag−Cu lead-free solder alloys containing La [J]. Transactions of Nonferrous Metals Society of China, 2007, 17: 1043−1048.

[14] CHEN K I, LIN K L. Effects of gallium on wettability, microstructures and mechanical properties of the Sn−Zn−Ag−Al−Ga solder alloys [C]//Proceedings of the 4th International Symposium on Electronic Materials and Packaging. Kaohsiung, Taibei, China: IEEE, 2002: 49−54.

[15] CHEN K I, CHENG S C, WU S, LIN K L. Effects of small additions of Ag, Al, and Ga on the structure and properties of the Sn−9Zn eutectic alloy [J]. Journal of Alloys and Compounds, 2006, 416: 98−105.

[16] ZHAO J, QI L, WANG X M, WANG L. Influence of Bi on microstructures evolution and mechanical properties in Sn−Ag−Cu lead-free solder [J]. Journal of Alloys and Compounds, 2004, 375: 196−201.

[17] RIZVI M J, CHAN Y C, BAILEY C, LU H, ISLAM M N. Effect of adding 1wt% Bi into the Sn−2.8Ag−0.5Cu solder alloy on the intermetallic formations with Cu-substrate during soldering and isothermal aging [J]. Journal of Alloys and Compounds, 2006, 407: 208−214.

[18] KANLAYASIRI K, MONGKOLWONGROJN M, ARIGA T. Influence of indium addition on characteristics of Sn−0.3Ag−0.7Cu solder alloy [J]. Journal of Alloys and Compounds, 2009, 485: 225−230.

[19] EL-DALY A A, FAWZY A, MOHAMAD A Z, EL-TAHER A M. Microstructural evolution and tensile properties of Sn−5Sb solder alloy containing small amount of Ag and Cu [J]. Journal Alloys and Compounds, 2011, 509: 4574−4582.

[20] YAN Y F, WANG Y S, FENG L F, SONG K X, WEN J B. Effect of Ag and Ni on the melting point and solderability of SnSbCu solder alloys [J]. International Journal of Minerals, Metallurgy and Materials, 2009, 16: 691−695.

[21] ESFANDYARPOUR M J, MAHMUDI R. Microstructure and tensile behavior of Sn−5Sb lead-free solder alloy containing Bi and Cu [J]. Materials Science and Engineering A, 2011, 530: 402−410.

[22] ZHANG C, LIU S D, QIAN G T, ZHOU J, XUE F. Effect of Sb content on properties of Sn−Bi solders [J]. Transactions of Nonferrous Metals Society of China, 2014, 24: 184−191.

[23] EL-DALY A A, HAMMAD A E, FAWZY A, NASRALLH D A. Microstructure, mechanical properties, and deformation behavior of Sn−1.0Ag−0.5Cu solder after Ni and Sb additions [J]. Materials and Design, 2013, 43: 40−49.

[24] CHEN W, XUE S, WANG H, HU Y. Effects of Ag on properties of Sn−9Zn lead-free solder [J]. Rare Metal Materials and Engineering, 2010, 39: 1702−1706.

[25] MOSER Z, SEBO P, GASIOR W, SVEC P, PSTRUS J. Effect of indium on wettability of Sn−Ag−Cu solders: Experiment vs. modeling, Part I [J]. Calphad, 2009, 33: 63−68.

[26] PIYAVATIN P, LOTHONGKUM G, LOHWONGWATANA B. Characterization of eutectic Sn−Cu solder alloy properties improved by additions of Ni, Co and In [J]. Materials Testing, 2012, 54: 383−389.

[27] ZHANG L, XUE S B, GAO L L, ZENG G, CHEN Y, YU S L. Creep behavior of SnAgCu solders with rare earth Ce doping [J]. Transactions of Nonferrous Metals Society of China, 2010, 20: 412−417.
[28] XUE S B, YU S L, WANG X Y, LIU L, HU Y F, YAO L H. Effects of rare earth element Ce on solderabilities of micron-powdered Sn−Ag−Cu solder [J]. Transactions of Nonferrous Metals Society of China, 2005, 15: 1285−1289.
[29] KANLAYASIRI K, ARIGA T. Physical properties of Sn58Bi−*x*Ni lead-free solder and its interfacial reaction with copper substrate [J]. Materials and Design, 2015, 86: 371−378.
[30] GAO F, QU J, TAKEMOTO T. Additives participation in Cu_6Sn_5 phase formed between Sn−3.5Ag solder and Cu by first-principle approach [C]//Proceedings of the 59th Electronic Components and Technology Conference. San Diego, California: IEEE, 2009: 1014−1020.
[31] HUH S H, KIM K S, SUGANUMA K. Effect of Ag addition on the microstructural and mechanical properties of Sn−Cu eutectic solder [J]. Materials Transactions, 2001, 42: 739−744.
[32] KARIYA Y, OTSUKA M. Effect of bismuth on the isothermal fatigue properties of Sn−3.5mass%Ag solder alloy [J]. Journal of Electronic Materials, 1998, 27: 866−870.
[33] MASSALSKI T B, OKAMOTO H, Binary alloy phase diagrams [M]. 2nd ed. Ohio: ASM International, 1990.
[34] EL-DALY A A, HAMMAD A E, AL-GANAINY G A, IBRAHIEM A A. Enhancing mechanical response of hypoeutectic Sn−6.5Zn solder alloy using Ni and Sb additions [J]. Materials and Design, 2013, 52: 966−973.
[35] GAO F, TAKEMOTO T, NISHIIKAWA H. Effects of Co and Ni addition on reactive diffusion between Sn−3.5Ag solder and Cu during soldering and annealing [J]. Materials Science and Engineering A, 2006, 420: 39−46.
[36] LEE Y G, DUH J G. Interfacial morphology and concentration profile in the unleaded solder/Cu joint assembly [J]. Journal of Materials Science: Materials in Electronics, 1999, 10: 33−43.
[37] YOON J W, KIM S W, JUNG S B. IMC morphology, interfacial reaction and joint reliability of Pb-free Sn−Ag−Cu solder on electrolytic Ni BGA substrate [J]. Journal of Alloys and Compounds, 2005, 392: 247−252.
[38] YANG M, LI M, WANG L, FU Y, KIM J, WENG L. Cu_6Sn_5 morphology transition and its effect on mechanical properties of eutectic Sn−Ag solder joints [J]. Journal of Electronic Materials, 2011, 40: 176−188.
[39] YANG G, YANG D, LI L. Microstructure and morphology of interfacial intermetallic compound $CoSn_3$ in Sn−Pb/Co−P solder joints [J]. Microelectronics Reliability, 2015, 55: 2403−2411.
[40] LIN S, HSU C, CHEN S, HSU C. Interfacial reactions in Sn−20In−2.8Ag/Cu couples [J]. Materials Chemistry and Physics, 2013, 142: 268−275.
[41] CHOI W, LEE H. Effect of soldering and aging time on interfacial microstructure and growth of intermetallic compounds between Sn−3.5Ag solder alloy and Cu substrate [J]. Journal of Electronic Materials, 2000, 29: 1207−1213.
[42] TSAO L C. Suppressing effect of 0.5wt.% nano-TiO_2 addition into Sn−3.5Ag−0.5Cu solder alloy on the intermetallic growth with Cu substrate during isothermal aging [J]. Journal of Alloys and Compounds, 2011, 509: 8441−8448.
[43] ANDERSON I E, COOK B A, HARRING J, TERPSTRA R L. Microstructural modifications and properties of Sn−Ag−Cu solder joints induced by alloying [J]. Journal of Electronic Materials, 2002, 31: 1166−1174.
[44] TSUKAMOTO H, DONG Z, HUANG H, NISHIMURA T, NOGITA K. Nanoindentation characterization of intermetallic compounds formed between Sn−Cu(−Ni) ball grid arrays and Cu substrates [J]. Materials Science and Engineering B, 2009, 164: 44−50.
[45] TSUKAMOTO H, NISHIMURA T, SUENAGA S, McDONALD S D, SWEATMAN K W, NOGITA K. The influence of solder composition on the impact strength of lead-free solder ball grid array joints [J]. Microelectronics Reliability, 2011, 51: 657−667.
[46] SHOHJI I, TSUNODA S, WATANABE H, ASAI T, NAGANO M. Reliability of solder joint with Sn−Ag−Cu−Ni−Ge lead-free alloy under heat exposure conditions [J]. Materials Transactions, 2005, 46: 2737−2744.
[47] SHOHJI I, WATANABE H, OKASHITA T, OSAWA T. Impact properties of lead-free Sn−Ag−Cu−Ni−Ge solder joint with Cu electrode [J]. Materials Transactions, 2008, 49: 1513−1517.
[48] ANDERSON I E, FOLEY J C, COOK B A, HARRINGA J, TERPSTRA R L, UNAL O. Alloying effects in near-eutectic Sn−Ag−Cu solder alloys for improved microstructural stability [J]. Journal of Electronic Materials, 2001, 30: 1050−1059.
[49] WANG Y W, LIN Y W, TU C T, KAO C R. Effects of minor Fe, Co, and Ni additions on the reaction between SnAgCu solder and Cu [J]. Journal of Alloys and Compounds, 2009, 478: 121−127.

Ag、Bi、In 和 Sb 添加对 Sn−0.6Cu−0.05Ni−Ge 无铅焊料性能的改变

Kannachai KANLAYASIRI, Rachata KONGCHAYASUKAWAT

Department of Industrial Engineering, Faculty of Engineering,
King Mongkut's Institute of Technology Ladkrabang, Bangkok 10520, Thailand

摘　要：对用于替换 Sn−Pb 共晶焊料的 Sn−Ag−Cu (SAC)焊料来说，Sn−Cu−Ni−Ge 焊料是一个巨大的挑战。本文作者研究添加 Ag、Bi、In 和 Sb 对 Sn−0.6Cu−0.05Ni−Ge (SCNG)无铅焊料物理性能的影响及与铜基体的界面反应。研究 SCNG−x 焊料的熔化行为、显微组织、抗拉强度和润湿性。结果表明，Ag、Bi、In 和 Sb 的引入对焊料的固相温度、液相温度和抗拉强度有微小的影响。但是，合金元素的浓度会影响焊料的冷却性能和凝固组织。除锑以外的合金元素的添加，提高了 SCNG 焊料的润湿性。合金元素的加入增加了金属间化合物层的厚度，这与焊料的冷却行为有关。SCNG−x 焊料与铜基体之间的金属间化合物层形貌与典型的 SAC 焊料不同。总之，用 Ag、Bi、In 或 Sb 对 SCNG 焊料进行合金化，可以改善焊料的特性。

关键词：Sn−Cu−Ni−Ge 焊料；无铅焊料；合金化效应；物理性能

(Edited by Wei-ping CHEN)